

GEOCHEMISTRY OF ACID MINE CONTAMINATION-AQUIFER INTERACTIONS

MARTHA CONKLIN, JOHN VILLINSKI and JOHN KAY

Department of Hydrology and Water Resources
The University of Arizona
Tucson, AZ, USA

Abstract. The Pinal Creek Basin near Globe, Arizona, is an example of a groundwater/surface water system contaminated by wastes from historic metal mining practices. Acidic mining wastes that have leached into the regional aquifer have come in contact with alluvial sediments, dissolving manganese oxides and precipitating iron sulfato-hydroxides. Manganese is reoxidized in sediments of a perennial stream (Pinal Creek) formed as the aquifer thins and groundwater is forced to land surface. Iron and manganese in the system are inextricably linked through redox couples. These interactions, which produce reaction rates varying by orders of magnitude and non-stoichiometric release of manganese, are poorly understood. We have designed a flow-through reaction cell to obtain *in situ* real time X-ray adsorption spectroscopy (XAS) data during geochemical reactions. By coupling solution chemistry data with spectroscopic measurements, we were able to show that the spinel mineral, jacobite, forms as a metastable intermediate phase during the reductive dissolution of manganese oxide (MnO₂) by ferrous iron (Fe(II)). The production of Fe(III) followed by the precipitation of ferric hydroxides and the formation of the jacobite phase, were responsible for reducing the rate of the reaction as time progressed. Laboratory studies have determined that Mn-oxidation in stream sediments increases Co, Ni, and Zn loading through a variety of processes, including oxidation, co-precipitation, solid solution formation, structural exchange, and/or sorption. This information provides a more complete picture of the controls on metal transport and attenuation in the Pinal Creek Basin.

Key words:

Acidic mining wasters, Manganese, Oxidation, Aquifer interactions

INTRODUCTION

Understanding the processes controlling the attenuation of metals by sediments in natural systems impacted by acid mine drainage is critical to the management and design of remediation efforts. The transport and fate of acid mine metal contaminants are often largely affected by existing and newly forming Fe, Al, and Mn-oxide sediment coatings [1]. These oxides provide efficient adsorption surfaces, and they can participate in oxidation-reduction reactions that change the stability and bonding of adsorbed species, in some cases leading to incorporation

within mineral structures [2,3]. Processes such as surface precipitation, solid solution formation, and microbially facilitated oxidation-reduction can substantially enhance trace metal accumulation at sediment surfaces [4–6]. In central Arizona, USA, the Pinal Creek Basin (Fig. 1) has been impacted by acid mine drainage from large scale copper mining activities during the last century. Low pH leachate (pH ~3) has infiltrated the alluvial aquifer underlying the basin resulting in the dissolution of natural aquifer materials and the subsequent release of metals, including Mn, Co, Ni, and Zn.

The paper presented at the Conference "Metal in Eastern and Central Europe: Health effects, sources of contamination and methods of remediation", Prague, Czech Republic, 8–10 November 2000.

This research was funded by the National Institute for Environmental Health Science (NIH P42 ESO4949) and the National Science Foundation (EAR-9523881). Address reprint requests to Dr M. Conklin, Department of Hydrology and Water Resources, The University of Arizona, Building 11, Rm 122, PO Box 210011, Tucson, AZ 85721-0011, USA.

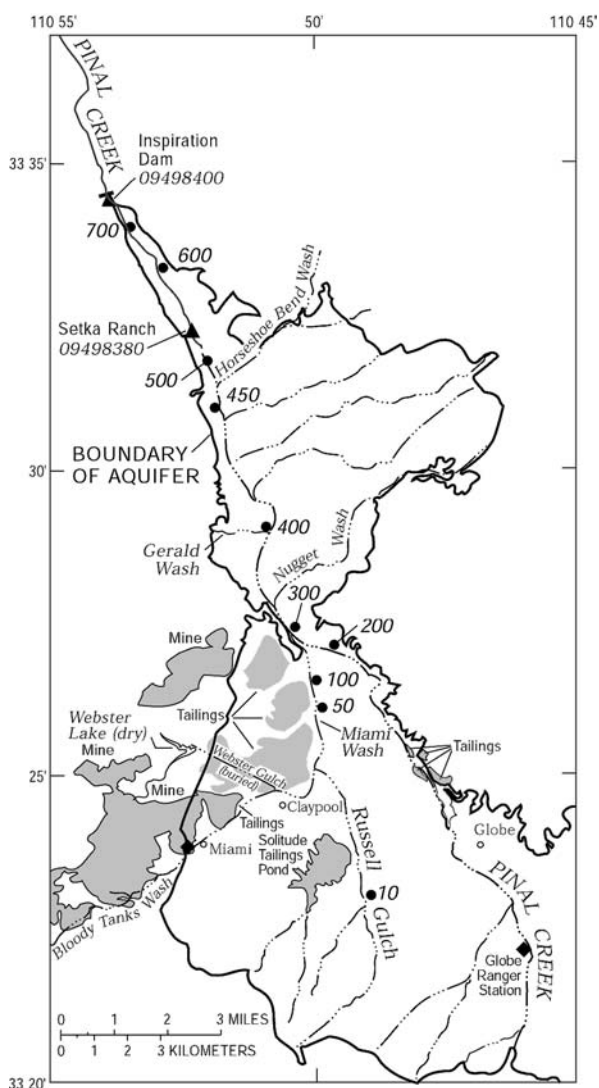


Fig. 1. Map of the Pinal Creek Basin. Low pH leachate originated in the general area of mine tailings in the west of the basin. Groundwater and surface water flow is from south to north.

In the Pinal Basin aquifer where there are sub-oxic conditions, aqueous Fe(II) is oxidized by Mn(III,IV)-hydroxides, resulting in the precipitation of Fe(III) sulfato-hydroxides and the release of aqueous Mn(II) [7], however, very little is known regarding the reaction mechanisms controlling Mn/Fe redox couples. Stollenwerk [8] performed column experiments on natural sediments and showed that less than 50% of the predicted manganese reduced by Fe(II) was released to solution. We have investigated the reductive dissolution of MnO₂ by Fe(II) under conditions simulating that of an acidic plume, resulting from mine wastes in real time by using an X-ray absorp-

tion spectroscopy (XAS) flow-through cell. Our goal was to determine if Mn intermediates form during reaction, and if so, to determine structural information regarding the intermediates.

Within the perennial reach of Pinal Creek where there are oxic conditions, Mn(II) released in the aquifer is reoxidized, resulting in the precipitation of Mn(III,IV)-hydroxides [9]. Newly forming Mn-oxides increase the attenuation of trace metals (Co, Ni, and Zn) by providing fresh sorption surfaces, and by facilitating oxidation, co-precipitation, solid solution, and ion exchange processes [10]. The primary objective of the research presented in this paper is to characterize the oxidation/reduction reactions in the aquifer controlling Fe and Mn transport, and to characterize the interaction of Mn, Co, Ni, and Zn with sediments in the perennial reach of Pinal Creek. This research is part of a multi-agency effort aimed at understanding the controls on metal transport in the Pinal Creek Basin, in order to assess the long term implications on ground and surface water quality. We refer to the experiments simulating aquifer conditions as the "sub-oxic experiments", and to the experiments simulating stream conditions as the "oxic experiments".

MATERIALS AND METHODS

Sub-oxic experiments. Batch experiments were performed under sub-oxic conditions (N₂-H₂ atmosphere) inside a glove box. All solutions contained less than 10 μg l⁻¹ of dissolved oxygen. Pyrolusite-coated quartz was equilibrated with inert electrolyte of similar composition to that of the acidic plume, with the exclusion of trace metals in order to focus on the Fe-Mn redox couples. The mixture was spiked with Fe(II) to yield initial concentrations of 4–10 mM Fe(II), pH was monitored continuously, and discrete samples were analyzed for Mn(II), Fe(II) and Fe_T.

Flow through cell experiments were performed at the Stanford Synchrotron Radiation Laboratory (SSRL), Stanford, CA, USA. A MnO₂-coated silica gel was used to increase the specific surface area of the MnO₂, thereby enhancing the ability to detect surface species during the

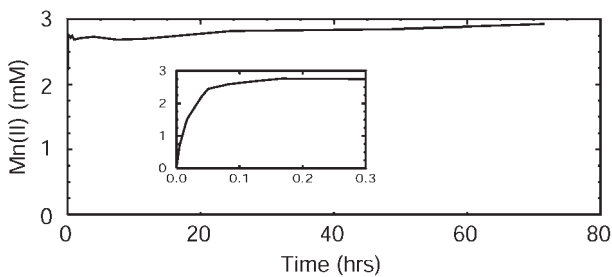


Fig. 2. Typical results of the release of Mn(II) to solution during batch experiment investigating the reductive dissolution of MnO_2 by Fe(II).

reaction. This material is referred to as $\text{MnO}_{2,\text{sc}}$. X-ray absorption near-edge structure (XANES) spectra were collected, pH was monitored, and the effluent was collected in set samples sizes and analyzed for Mn(II) and total iron (Fe_T). XANES reaction spectra were fit with linear combinations of XANES spectra of reference Mn minerals using the non-linear, least-squares routine in EXAFS-PAK [11]. Details of the experimental setup have been described elsewhere [12].

Oxic experiments. To examine the interactions of Mn, Co, Ni, and Zn with sediments in the perennial reach of Pinal Creek, we conducted a series of column experiments using contaminated sediments collected from the streambed. Uptake experiments were conducted for 450 pore volumes, at which point a metal free solution was eluted for 150 pore volumes to examine metal release. An artificial stream water (ASW) with major ion and Mn, Co, Ni, and Zn concentrations ($55, 0.57, 0.77, 1.2 \text{ mg L}^{-1}$) similar to surface water at Pinal Creek [13] was used in all uptake experiments. ASW without Mn, Ni, Co, or Zn was used in desorption experiments. Two experiments were conducted, biotic and abiotic. Biotic experiments contained naturally occurring Mn-oxidizing bacteria, and most closely represented stream conditions. Abiotic conditions were achieved by poisoning biotic sediments to eliminate Mn-oxidizing bacteria. The difference between biotic and abiotic experiments represents the effect of microbial Mn-oxidation. Each experiment was conducted using three sediments of different Mn-oxide content to examine the relative effect of pre-existing Mn-oxide content on metal uptake and retention. Uptake, release, and retention were determined from breakthrough curves.

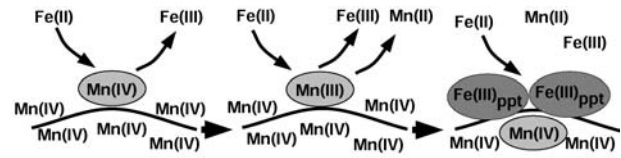


Fig. 3. General conceptual model of the inhibition of the reductive dissolution of MnO_2 by Fe(II) due to the ferric precipitates coating available Mn(IV) surface sites.

Breakthrough curves were modeled using a one-dimensional solute transport parameter estimation code CXTFIT (14) to determine rate constants for continuous uptake.

RESULTS AND DISCUSSION

Sub-oxic experiments. Typical results of the Mn(II) release to solution in the batch experiments are presented in Fig. 2. The release of Mn(II) solution was typified by an initial fast release in the first 10–15 min of the experiment, followed by a much slower release over a period of days. This change in reaction rate coincided with the decrease of Fe(III) in solution and the concomitant consumption of protons due to Fe(III) sorption and precipitation (presumably as $\text{Fe}(\text{OH})_3$). Therefore, we postulated that the decrease in the reaction rate was due to coating of Mn(IV) surface sites by a ferric precipitate (Fig. 3). Mass balance results indicate that Mn is not released in stoichiometric proportions to the amount of Fe(II) oxidized, however, the magnitude of the imbalance is not as great as that found by Stollenwerk [8].

Flow through cell experiments were performed at SSRL to probe the reaction *in situ*, with the intent to determine the manganese speciation as the reaction progressed. Spectroscopic results (Fig. 4) indicate that the Mn(II) is released to solution as is evidenced by the increased magnitude of the shoulder at 6554 eV. In addition, the energy of maximum absorption decreases from 6561.5 to 6560 eV, indicating that the average valence of the manganese in the sample has decreased. A second shoulder at 6549 eV appears and cannot be attributed to either manganese end member ($\text{MnO}_{2,\text{sc}}$ or $\text{Mn}(\text{II})_{\text{aq}}$). Furthermore, a peak appears in the pre-edge region (Fig. 4, inset). This feature

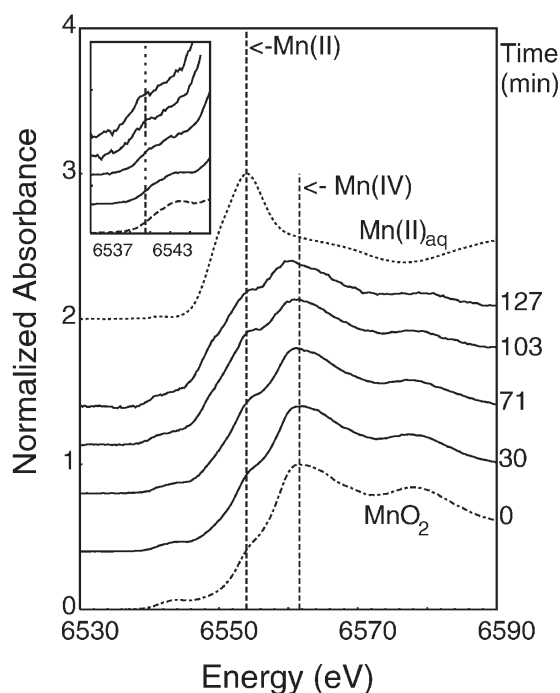


Fig. 4. XANES spectra collected during reductive dissolution of $\text{MnO}_{2,\text{sc}}$ by Fe(II) . The data have been normalized to an edge height of one and vertically offset for clarity. Approximately every other scan has been plotted. Inset is a blow-up of the pre-edge region; times are the same.

is generally attributed to forbidden 1s-3d transitions, thought to be allowed when there is a decrease in the symmetry of the Mn environment [15]. This can be due to either tetrahedral coordination or the presence of Mn(III) which distorts the bond lengths in the octahedral coordination due to Jahn-Teller effects.

Fits of the reaction spectra with the two manganese end members ($\text{MnO}_{2,\text{sc}}$ and $\text{Mn(II)}_{\text{aq}}$) were increasingly unsatisfactory as the reaction progressed. A third component was added to the fit, and jacobsite, MnFe_2O_4 was the only Mn(II,III) mineral that adequately fit the data. Results from one XANES spectrum, and the fits with and without jacobsite, are presented in Fig. 5. The first derivatives of the spectrum and the fits are presented to highlight the differences in the fits. Concentration is linearly related to absorbance as a first approximation. Approximately 5% of the original Mn(IV) was present in the jacobsite intermediate phase after two hours of reaction. While this value is smaller than the 50% imbalance found by Stollenwerk [8], our system is less complex, a fact which may account for a lower Mn imbalance.

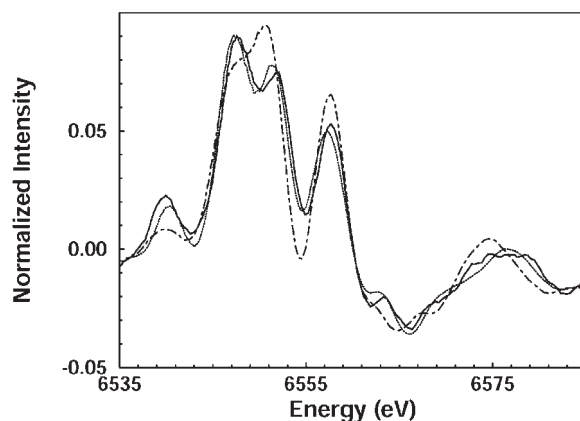


Fig. 5. Fit results of a sample XANES reaction spectrum. First derivatives of the spectrum and fits are presented to highlight differences. (—) is the reaction spectrum, (- - -) is the fit with $\text{Mn(II)}_{\text{aq}}$ and $\text{MnO}_{2,\text{sc}}$, and (.....) is the fit that also included jacobsite (MnFe_2O_4).

Oxic experiments. Typical breakthrough curves from column experiments simulating stream conditions are presented in Fig. 6. Mn(II) uptake reached complete breakthrough ($C/C_0 = 1$) within 100 pore volumes, and was best modeled as an equilibrium process (Fig. 6). Mn uptake was 8 ± 7 , 39 ± 9 , and $9 \pm 7\%$ higher in biotic experiments than abiotic experiments for the low, intermediate, and high sediments, respectively, consistent with previous investigations which observed enhanced Mn-oxidation due to microbial facilitation [16–18]. Retention of Mn was 392 ± 32 , 124 ± 14 , and $5 \pm 7\%$ higher under biotic conditions for the low, intermediate, and high sediments respectively, indicating that microbial oxidation decreased in importance relative to abiotic oxidation as sediment Mn-oxide content increased. Although initial uptake of Mn occurred primarily as adsorption, the majority of Mn retained in columns was incorporated into Mn-oxides. These results suggest initial uptake of Mn by adsorption, followed by surface oxidation of adsorbed Mn(II) to form Mn(III, IV) oxides, as has been previously proposed [19,20].

As with Mn, Ni reached complete breakthrough within 100 pore volumes (Fig. 6). Ni uptake under all experimental conditions was best modeled with equilibrium assumptions, consistent with adsorption as the primary uptake mechanism. The adsorption of nickel onto Mn-oxides has been observed by numerous previous investigators [19,21,22]. Ni uptake in biotic columns was 81 ± 11 , 88

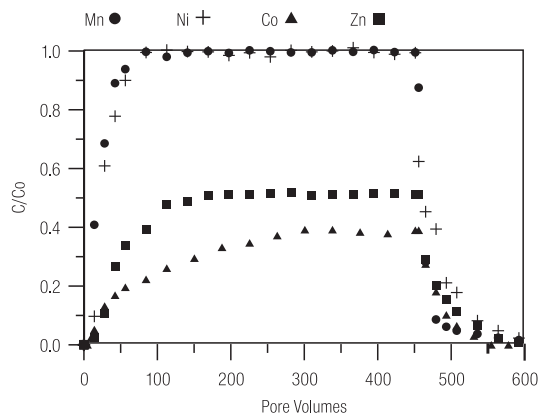


Fig. 6. Typical breakthrough curves from biotic experiments for Mn, Co, Ni, and Zn. Mn and Ni reached complete breakthrough, while Co and Zn reached a plateau beneath complete breakthrough, indicating a mechanism of continuous uptake.

± 11 , and $90 \pm 12\%$ higher than in abiotic columns for the low, intermediate, and high sediments, respectively. The difference between biotic and abiotic Ni uptake is attributed to adsorption onto newly formed Mn-oxide surfaces, which is consistent with observed Ni uptake in the hyporheic zone at Pinal Creek [13].

Unlike Mn and Ni, Co did not reach complete breakthrough ($C/C_0 = 1$). Continuous uptake of Co was evident from the plateau behavior exhibited by breakthrough curves (Fig. 6). The amount of continuous uptake increased with increasing sediment Mn-oxide content, resulting in approximately 8, 30, and $65 \pm 5\%$ removal of the influent Co under biotic conditions for the low, intermediate, and high sediments, respectively. Uptake of Co in the biotic experiment was 42 ± 8 , 29 ± 8 , and $75 \pm 11\%$ greater than uptake in the abiotic experiment for the low, intermediate, and high Mn-oxide sediments, respectively. Direct microbial oxidation of Co in Pinal Creek sediments was not observed in batch experiments [23], therefore, it is assumed that microbially enhanced uptake of Co was due to increased Mn oxidation. Oxidation of adsorbed Co(II) to Co(III) on Mn-oxides and incorporation into the Mn-oxide structure has been proposed as an explanation of large amounts of Co uptake onto Mn-oxides [21,24,25].

In sharp contrast to Co, Mn, and Ni, Zn uptake and retention were minimally affected by microbial Mn-oxidation or pre-existing sediment Mn-oxide content. During the first

100 pore volumes breakthrough was best modeled as equilibrium, but Zn breakthrough reached a plateau of approximately $C/C_0 = 0.55$, indicating a mechanism of continuous uptake (Fig. 6). The fact that Zn uptake was largely independent of newly forming or existing Mn-oxides suggests that a continuous uptake occurred during precipitation of a new Zn mineral phase, however, Zn was undersaturated with respect to common pure phase minerals. It is suspected that Zn participated in the formation of a solid solution. Manganese in column experiments was supersaturated with respect to the oxide phases hetaerolite ($ZnMn_2O_4$; log SI = 11.62) and hausmannite (Mn_3O_4 ; log SI = 12.30). Hetaerolite can preferably form over hausmannite when Zn(II) is more stable than Mn(II), which was the case in these experiments [26]. Mn was also supersaturated with respect to rhodochrosite ($MnCO_3$, SI = 0.70), and Zn was near saturation with respect to smithsonite ($ZnCO_3$, SI = -1.54). Rhodochrosite-smithsonite solid-solution series have been observed to form at low temperatures in solutions supersaturated with Mn^{2+} and undersaturated with Zn^{2+} [27].

Large scale irreversible geochemical changes in the Pinal Basin aquifer have resulted in substantial loading of metals in the oxic stream bed of Pinal Creek. Although the sub-oxic and oxic environments are hydrologically connected, they are geochemically very different. A wide range of mechanisms affected metal transport and attenuation, with oxidation-reduction conditions acting as primary control. The specific mechanisms controlling metal uptake and release were not always intuitive or easy to predict without considering each metal on an individual basis, as exemplified by the low temperature spinel formation we observed. Understanding the behavior of metals in the aquifer and stream facilitates our ability to model and predict transport and fate of contaminants in systems similar to Pinal Basin.

ACKNOWLEDGEMENTS

The authors wish to acknowledge that the comments from the reviewers, Tim Corley and Jungyill Choi are greatly appreciated.

REFERENCES

1. Dzombak DA, Morel FM. *Adsorption of inorganic pollutants in aquatic systems*. J Hydrologic Engineering 1987; 113: 430–75.
2. Davis JA, Kent DB. *Surface complexation modeling in aqueous geochemistry*. In: Hochella MF, White AF, editors. *Mineral-Water Interface Geochemistry*. Vol. 23. Reviews in Mineralogy. Washington, DC: Mineralogical Soc. of Am; 1990. p. 177–260.
3. Hem JD. *Redox processes at surfaces of manganese oxides and their effects on aqueous metal ions*. Chem Geol 1978; 21: 199–218.
4. Hem JD. *Rates of manganese oxidation in aqueous systems*. Geochim Cosmochim Acta 1981; 45: 1369–74.
5. Stumm W, Morgan JJ. *Aquatic Chemistry; Chemical Equilibria and Rates in Natural Waters*. III ed. Chapter 9. New York: Wiley and Sons; 1996.
6. Ehrlich HL. *Geomicrobiology*. New York: Marcel Dekker; 1996.
7. Villinski JE. *Reductive dissolution of manganese(IV) oxides and precipitation of ferric iron: implications for redox processes in an alluvial aquifer affected by acid mine drainage* [Ph.D dissertation]. The University of Arizona; 2001.
8. Stollenwerk, Kenneth G. *Geochemical interactions between constituents in acidic groundwater and alluvium in an aquifer near Globe, Arizona*. Appl Geochem 1994; 9: 353–69.
9. Harvey JW, Fuller CC. *Effect of enhanced manganese oxidation in the hyporheic zone on basin-scale geochemical mass balance*. Water Resour Res 1998; 34: 623–36.
10. Kay JT. *The reactive uptake and release of Mn(II), Co(II), Ni(II) and Zn(II) by sediments from a mining-contaminated stream, Pinal Creek, Arizona*. [Master's Thesis]. The University of Arizona, 2000.
11. George GN. *EXAFSPAK: A suite of computer programs for analysis of X-ray absorption spectra*. Stanford, CA: Stanford Synchrotron Radiation Laboratory; 1993.
12. Villinski JE, O'Day PA, Corley TL, Conklin MH. *In situ spectroscopic and solution analyses of the reductive dissolution of MnO₂ by Fe(II)*. Environ Sci Technol 2001; 35: 1157.
13. Fuller CC, Harvey JW. *Reactive uptake of trace metals in hyporheic zone of a mining-contaminated stream*. Environ Sci Technol 2000; 34: 1150–60.
14. Toride N, Leij FJ, van Genuchten M. *The CXTFIT code for estimating transport parameter from laboratory or field tracer experiments*. US Salinity Laboratory Report 1995; 137.
15. Manceau A, Gorshkov AI, Drits VA. *Structural chemistry of Mn, Fe, Co, and Ni in manganese hydrous oxides: I. Information from XANES spectroscopy*. Amer Miner 1992; 77: 1133–43.
16. Diem D, Stumm W. *Is dissolved Mn²⁺ being oxidized by O₂ in the absence of Mn-bacteria or surface catalysts?* Geochim Cosmochim Acta 1989; 48: 1571–3.
17. Nealson KH, Ford J. *Surface enhancement of bacterial manganese oxidation; implications for aquatic environments*. Geomicrobiol J 1980; 2: 21–37.
18. Marble JC. *Biotic contribution of Mn(II) removal at Pinal Creek, Globe, Arizona* [Master's Thesis]. Tucson, AZ: University of Arizona; 1998.
19. Tamura H, Furuichi R. *Adsorption affinity of divalent heavy metal ions for metal oxides evaluated by modeling with the Frumkin isotherm*. J Colloid Interface Sci 1997; 195: 241–9.
20. Posselt HS, Anderson FJ. *Cation sorption on colloidal hydrous manganese dioxide*. Environ Sci Technol 1968; 2: 1087–93.
21. Davies SH, Morgan JJ. *Manganese(II) oxidation kinetics on metal oxide surfaces*. J Colloid Interface Sci 1989; 129: 63–77.
22. Murray JW. *The interaction of metal ions at the manganese dioxide-dissolution interface*. Geochim Cosmochim Acta 1975; 39: 505–19.
23. Flinchbaugh H. *Biotic and abiotic processes contributing to the removal of Mn(II), Co(II) and Cd(II) from Pinal Creek, Globe, Arizona*. [Master's Thesis]. Tucson, AZ: University of Arizona, Department of Hydrology and Water Resources; 1996.
24. Loganathan P, Bureau RG. *Sorption of heavy metal ions by a hydrous manganese oxide*. Geochim Cosmochim Acta 1973; 37: 1277–93.
25. Burns RG. *The uptake of cobalt into ferromanganese nodules, soils, and synthetic manganese(IV) oxides*. Geochim Cosmochim Acta 1976; 40: 95–102.
26. Hem JD, Roberson CE, Lind CJ. *Synthesis and stability of heteroite, ZnMn₂O₄, at 25°C*. Geochimica Cosmochimica Acta 1987; 51: 1539–47.
27. Bottcher ME, Gehlken PL, Birch WD, Usdowski E, Heofs J. *The rhodochrosite smithsonite solid-solution series from broken-hill (NSW), Australia-geochemical and infrared spectroscopic investigations*. N Jb Miner Mh 1993; 8: 352–62.

Received for publication: January 25, 2001

Approved for publication: August 20, 2001